Available online at www.sciencedirect.com
ScienceDirect
Journal of Catalysis 246 (2007) 66–73
JOURNAL OF CATALYSIS
www.elsevier.com/locate/jcat

In situ ATR-IR study of CO adsorption and oxidation over Pt/Al_2O_3 in gas and aqueous phase: Promotion effects by water and pH

Sune D. Ebbesen, Barbara L. Mojet, Leon Lefferts *

Catalytic Processes and Materials, Faculty of Science and Technology, Institute of Mechanics Processes and Control Twente (IMPACT), University of Twente, P.O. Box 217, 7500 AE, Enschede, The Netherlands

Received 9 June 2006; revised 25 September 2006; accepted 18 November 2006

Available online 22 December 2006

Abstract

The adsorption and oxidation of carbon monoxide over a Pt/Al_2O_3 catalyst layer deposited on a ZnSe internal reflection element was investigated both in gas phase and water using attenuated total reflection infrared spectroscopy. A preparation method is described that results in a strongly attached layer that is stable for many days in a water flow. Both adsorption and oxidation of CO are largely affected by the presence of liquid water. It influences the metal particle potential as well as the CO molecule directly, which is reflected in large red shifts (45 cm^{-1}) and a fourfold higher intensity when the experiments are carried out in water. Furthermore, the rate of CO oxidation changes significantly when carried out in water compared with gas phase. Finally, with increasing pH, CO stretching frequencies shift to lower wavenumbers, accompanied by a large increase in CO oxidation rate.

Keywords: ATR-IR spectroscopy; CO oxidation; Carbon monoxide; Adsorption; Pt/Al_2O_3; Liquid phase; Water; pH effect

1. Introduction

The chemical industry is continuously searching for more cost- and performance-efficient processes, and thus the trend is toward using water as a solvent. The selection of water as a solvent offers many benefits, including low cost, environmental friendliness, availability, and safety. The chemical industry is nevertheless a major contributor to environmental pollution, largely due to the use of hazardous solvents. Of the top 10 chemicals released or disposed of by the chemical industry in the mid-1990s, five were solvents: namely, methanol, toluene, xylene, methyl ethyl ketone, and methylene chloride [1].

For this reason, also catalytic wastewater and groundwater treatments are receiving increasing attention. Water purification in general includes especially oxidation processes and to a lesser extent, hydrogenation processes as well [2]. As an example, over several catalysts, wet-air oxidation can be applied for removal of organic compounds from water [2]. Denitrification (nitrite and nitrate removal) is one of the most investigated hydrogenation reactions in groundwater treatment. The denitrification is catalyzed by supported bimetallic noble metals [3]. Technology in this area is developing, and at the current stage the formation of ammonia as a side product is a problem because it is undesirable in drinking water [4]. The selectivity to nitrogen is known to depend on, among other things, the type of reducing agent or pH.

So far, detailed mechanistic studies are lacking, because it is difficult to study heterogeneous catalysts *in situ* if the reaction is carried out in water. In gas phase, vibrational spectroscopy is a versatile tool for studying adsorption and reaction on catalytic surfaces. However, in liquid-phase reactions, application of normal transmission infrared spectroscopy is not suitable unless the path length of the light is very short (i.e., in the order of a few microns), because liquids (particularly water) normally are strong absorbers of infrared radiation. Attenuated total reflection infrared spectroscopy (ATR-IR), however, is ideally suited for studying molecular vibrations at the solid–liquid interface, because the evanescent wave is restricted to the region near the interface, thereby minimizing the contribution from the liquid [5]. As a result, the correct design of the ATR cell allows

* Corresponding author. Fax: +31 53 489 4683.
E-mail addresses: s.d.ebbesen@utwente.nl (S.D. Ebbesen), b.l.mojet@utwente.nl (B.L. Mojet), l.lefferts@utwente.nl (L. Lefferts).

0021-9517/$ – see front matter
doi:10.1016/j.jcat.2006.11.019

for good mimicry of a normal liquid-phase heterogeneous catalytic experiment, because mass transfer is not hampered by a very thin liquid layer. Only recently, ATR-IR spectroscopic studies at the metal–liquid interface have begun to receive attention [6–12]. For example, the adsorption and oxidation of CO and dissociation of small molecules, such as formaldehyde, over Pt/Al_2O_3 catalysts has been reported [11]. In addition, ATR-IR spectroscopic studies of the water–gas shift reaction and methanol reforming over Pt/Al_2O_3 wave been combined with kinetic studies [9]. In our lab, we showed the significant effect of water on the oxidation rate of CO compared with gas-phase CO oxidation over Pt/ZnSe [7]. CO is a widely applied molecule for characterizing supported noble metal catalysts [13–24]. Interactions between CO and the active metal are reflected in shifts of the CO absorption bands, which in turn are known to be affected by metal–support interactions. Because the vibrations are so sensitive for modifications of the metal particles and/or its surrounding medium, CO is an ideal model compound for characterizing supported noble metal catalysts. In addition, CO oxidation is a very simple reaction that allows for a detailed *in situ* study of reaction parameters, such as the effect of solvent or pH.

Especially the details of the influence of pH on heterogeneous catalytic reactions in water have not been resolved completely. For this reason, the objective of this study is to unravel the details of the influence of water and the pH on the CO adsorption and oxidation on Pt/Al_2O_3 using *in situ* ATR-IR spectroscopy.

2. Experimental

2.1. Catalyst preparation

Pt/Al_2O_3 was prepared by wet impregnation according to the following procedure. Al_2O_3 (Aluminum oxide C, Degussa, primary particle size 13 nm) was precalcined for 5 h at 823 K (heating/cooling rate, 5 K/min) in stagnant air. The powder was then impregnated with a solution of $H_2PtCl_6 \cdot 6H_2O$ (Alfa Aesar) to yield a catalyst with 5 wt% metal loading. The catalyst solution was mixed for 2 h, followed by drying at 335 K overnight in a rotating evaporator. The impregnated Pt/Al_2O_3 powder was calcined at 673 K for 3 h (heating rate, 5 K/min) in flowing synthetic air (30 mL/min). Subsequently, the calcined catalyst was reduced at 673 K for 3 h (heating rate, 5 K/min) in flowing hydrogen (30 mL/min).

A suspension of the catalyst was prepared from 0.3 g of catalyst and 50 mL of water, with pH adjusted to 3.5 with nitric acid to stabilize the small alumina particles. The suspension was milled for 1 h (Fritsch Pulverisette) to break up any agglomerates and obtain nanometer-sized catalyst particles. For immobilization of the catalyst layer, colloidal alumina (Aluminum oxide, 20% in H_2O colloidal suspension, Alfa Aesar, particle size 5 nm) was added (which is the general methodology of preparing washcoats in monolithic catalysts) [25] to create a catalyst suspension containing 5 wt% colloidal alumina. The catalyst layer was prepared on the internal reflection element (IRE) by adding 1 mL of the suspension onto a ZnSe IRE. The suspension was allowed to evaporate overnight at room temperature. Subsequently, the catalyst layer/IRE was calcined at 573 K for 2 h (heating/cooling rate, 1 K/min) in flowing synthetic air (30 mL/min) and reduced at 573 K for 2 h (heating/cooling rate, 1 K/min) in flowing hydrogen, followed by heating to 673 K in hydrogen (heating rate, 10 K/min) to ensure removal of all NO_x species (originating from the nitric acid that used as a stabilizer) from the catalyst. After calcination and reduction the catalyst layer was slowly exposed to air and ready for use. The amount of catalyst deposited on the IRE was approximately 6 mg.

2.2. Catalyst characterization

BET specific surface area of the powders was measured by N_2 adsorption–desorption at 77 K in an ASAP 2400 (Micromeritics) instrument. Platinum dispersion was determined by H_2 chemisorption with 0.2 g of catalyst in a home-built volumetric system. The sample was reduced at 473 K in H_2 for 1 h. After reduction, the sample was degassed at 473 K in vacuum (10^{-6} mbar). The sample was cooled to room temperature (293 K) and the H_2 adsorption isotherm was measured by introducing H_2 to the sample. After the first isotherm, the sample was degassed at room temperature, followed by a second H_2 adsorption isotherm. The hydrogen chemisorption capacity was calculated by extrapolation of the hydrogen uptake to zero pressure, which corresponded to the difference of the first and second isotherms [26].

The structure of the prepared catalyst layer was studied with scanning electron microscope (LEO 1550 FEG SEM).

2.3. In situ ATR-IR spectroscopy

ATR-IR spectra were recorded using a homebuilt stainless steel flowthrough cell as described in detail elsewhere [7]. The cell was mounted within the sample compartment of an infrared spectrometer (Bruker Tensor 27) equipped with a MCT detector. All ATR-IR spectra were recorded at room temperature (294 K) in an air-conditioned room. Infrared spectra were recorded by averaging of 128 scans with a resolution of 4 cm^{-1}. Correction of the spectra for water absorption is performed by subtraction of a scaled water background, chosen by a fit to the spectrum, as recently published by our group [7].

After being assembled in the IR spectrometer, the cell was purged with gaseous argon, followed by a reducing gas flow for 2 h (10% H_2/Ar) to remove surface oxygen. Then adsorption experiments were performed. For experiments in aqueous phase, the catalyst was reduced in hydrogen-saturated Q2 water (7.8×10^{-5} mol H_2/L) before adsorption experiments. Q2 water (prepared using the Millipore Milli-Q water treatment system from Amphotech Ltd.) was used for all experiments. Aqueous flow was regulated by a belt pump (Watson Marlow 503s) mounted downstream of the ATR-IR cell; all aqueous flow rates were 1 mL/min, resulting in a residence time of 7.2 s. Saturation of water with 1% CO/Ar (5.0, Praxair), Ar (5.0, Praxair), 10% O_2/Ar (5.0, Praxair), or H_2 (5.0, Praxair), was performed at room temperature (294 K) with gas flow rates of 40 mL/min. The concentrations of dissolved gases in water were calculated

based on reported solubility data at room temperature and gas pressure of 1 atm.

3. Results

3.1. Catalyst characterization

The specific surface area as determined by N_2 physisorption of the Al_2O_3 support powder was 125 m^2/g after calcination at 823 K. After subsequent impregnation, calcination and reduction at 673 K, the Pt/Al_2O_3 powder sample had a surface area of 115 m^2/g. The hydrogen chemisorption capacity (H/Pt) was 0.75. To measure the thickness of the catalyst layer deposited on the IRE, a catalyst layer was prepared on a glass plate with the same catalyst amount and surface area as on the IRE used for the ATR-IR experiments. The glass plate was cut through (from the back side) using a diamond cutter, and the catalyst layer was carefully broken and studied by SEM. Fig. 1 shows typical SEM micrographs of the Pt/Al_2O_3 catalyst layer on a glass plate. The layer was smooth on the nanometer-length scale and consisted of small particles (approximately 20–30 nm), no distinction between alumina and platinum particles can be made due to the high platinum dispersion. The thickness of the catalyst layer was measured to be 3.50 ± 0.25 μm over the full length of the plate. Thinner layers that remained stable during reactions could not be prepared.

In addition, the transmission and the ATR spectra of CO adsorbed in the gas phase on, respectively, the powder catalyst and the thin catalyst layer were identical, as given in the supporting information. This clearly demonstrates that the experimental procedure to produce a thin layer of catalyst on the ZnSe crystal does not affect the catalytically active platinum particles.

3.2. In situ ATR-IR measurements

3.2.1. Adsorption of CO from gas and aqueous phase

After assembling the ATR-IR cell and reducing the catalyst layer (see Section 2), dry gas-phase CO was introduced into the cell. Fig. 2 shows the ATR-IR spectra obtained during CO flow over Pt/Al_2O_3.

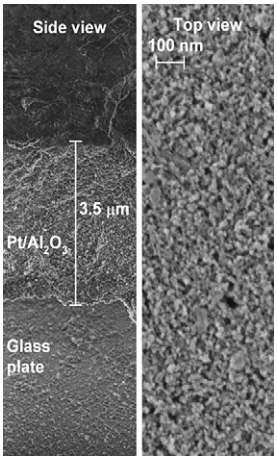

Fig. 1. SEM micrographs of a Pt/Al_2O_3 layer on a glass plate with identical dimensions as the ZnSe IRE (left: side view and right: top view).

No gaseous CO was detected during CO flow, whereas linearly adsorbed CO on platinum was initially detected with a distinct asymmetric infrared peak appearing at 2065 cm^{-1}, which shifted to 2071 cm^{-1}, due to dipole–dipole coupling with increasing surface coverage [27,28] at saturation level after 5 min. Because the CO concentration was low, this time was needed to dose the stoichiometric amount of CO for the platinum particles to adsorb; it is not the result of diffusion limitations within the catalyst layer. Bridging CO on platinum was identified by a very broad, low-intensity peak between 1750 and 1900 cm^{-1}. Peak positions for both linear and bridging CO on Pt/Al_2O_3 are similar to positions reported in the literature [15,28–30]. After a flow of dry CO, the cell was flushed with dry argon for 15 min, after which a dry oxygen-rich stream (10% O_2/Ar) was introduced to oxidize the adsorbed CO. CO was only partly removed during oxidation at room temperature (see also Section 3.2.2). To allow reuse of the catalyst layer, the IRE with catalyst was oxidized *ex situ* at 523 K for 2 h in flowing synthetic air (30 mL/min, at a heating/cooling rate of 1 K/min), followed by reduction at 523 K for 2 h in flowing hydrogen (30 mL/min, at a heating/cooling rate of 1 K/min), exposed to air, and mounted in the ATR-IR cell. Subsequently, the cell was purged with gaseous argon (15 min), followed by reduction for 2 h (10% H_2/Ar) to remove surface oxygen. Subsequently,

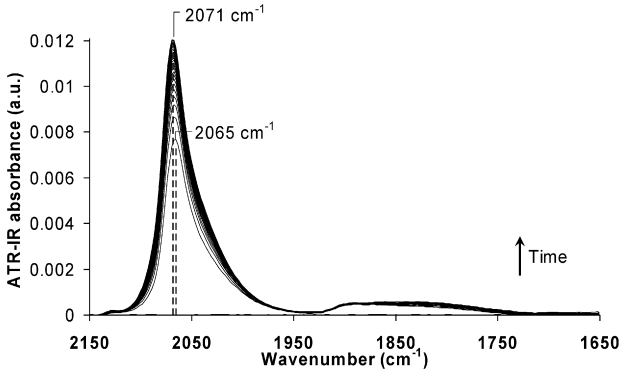

Fig. 2. ATR-IR spectra as a function of time (time interval: 1.5 min) showing the region of CO adsorption on Pt/Al_2O_3 while dry CO was flown (1% CO/Ar).

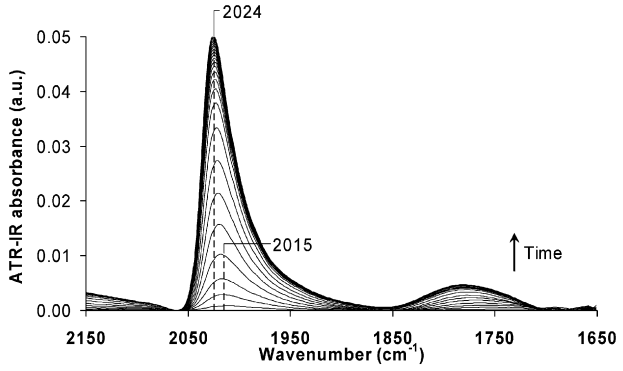

Fig. 3. Water corrected ATR-IR spectra as a function of time (time interval of 1.5 min) showing the region of CO adsorption on Pt/Al_2O_3 while CO in water (1.4×10^{-6} mol CO/L) was flown at pH 6.9. Note the four times higher infrared intensity for adsorbed CO as compared to adsorption from gas phase (Fig. 2).

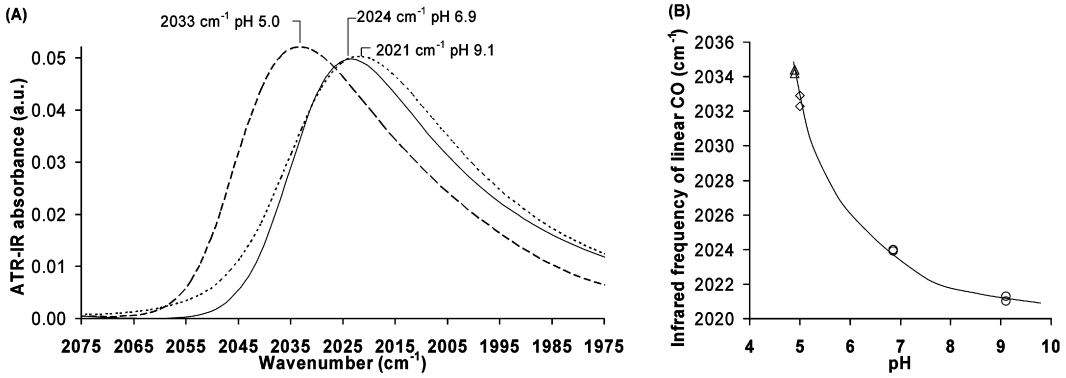

Fig. 4. (A) Water corrected ATR-IR spectra of linearly adsorbed CO on Pt/Al_2O_3 while CO in aqueous phase (1.4×10^{-6} mol CO/L) at different pH was flown, and (B) ATR-IR frequency of linearly adsorbed CO on Pt/Al_2O_3 in aqueous phase as a function of pH ((△) adjusted with H_3PO_4, (◇) adjusted with H_2SO_4, (○) adjusted with NaOH).

hydrogen-saturated Q2 water (7.8×10^{-5} mol H_2/L) was introduced (until a stable background was obtained, which took several hours), followed by a flow of Q2 water at pH 6.9 saturated with CO (1.4×10^{-6} mol CO/L), and ATR-IR spectra were collected (Fig. 3).

When adsorbed from aqueous phase, linear CO was initially detected by a peak at 2015 cm^{-1}; this shifted to 2024 cm^{-1} at increasing coverage, due to dipole–dipole coupling [27,28]. Bridging CO was detected by a very broad peak with a maximum around 1780 cm^{-1}. During subsequent flow of pure Q2 water, the intensity of the bands for both linear and bridging CO remained constant, indicating that the layer with adsorbed CO remained stable. After flowing water, the adsorbed CO was oxidized by oxygen in Q2 water (1.3×10^{-4} mol O_2/L) to remove all CO (see also Section 3.2.2). Subsequently, the catalyst layer was reduced *in situ* by hydrogen in water (7.8×10^{-5} mol H_2/L) for several hours to repeat experiments. Repetition of experiments showed that the oxidation/reduction treatment to clean the catalyst from CO had no influence on the observed CO spectra. This was particularly important, because this allowed comparison of intensities of different experiments on the same Pt/Al_2O_3 sample.

In addition, the effect of pH on CO adsorption in aqueous phase was examined. CO in Q2 water at pH 4.9, 5.0, 6.9, and 9.1 (pH adjusted with either H_2SO_4, H_3PO_4, or NaOH) was flown over the same Pt/Al_2O_3 catalyst layer as used for CO adsorption in gas and aqueous phases, and ATR-IR spectra were recorded (Fig. 4). After each adsorption experiment, adsorbed CO was oxidized by introducing oxygen in water (1.3×10^{-4} mol O_2/L) at the same pH as during CO adsorption; as a result, CO was removed completely. After oxidation, the catalyst layer was reduced *in situ* by hydrogen in water as described above.

Figs. 4A and 4B clearly show a shift of 12 cm^{-1} to lower wave number with increasing pH from 5.0 to 9.1 for the band of linearly adsorbed CO. Likewise, shifts were found for bridging CO (not shown), but because of the very broad peaks, the exact peak positions could not be reliably determined. At pH 5, we find no significant differences in peak position between H_3PO_4 and H_2SO_4 solutions, indicating an insignificant influence of the counter ion compared with that of pH. Although peaks clearly shifted with changing pH, only slight differences in the linear-to-bridge ratio were observed, and no relation between pH and the linear-to-bridge ratio could be determined.

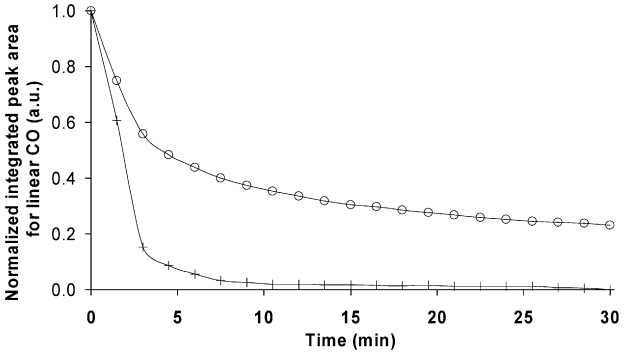

Fig. 5. Normalized integrated peak area of linear CO adsorbed on Pt/Al_2O_3 versus time during oxidation from gas (○) and aqueous phase at pH 6.9 (+).

3.2.2. *Oxidation of preadsorbed CO*

After CO adsorption on the Pt/Al_2O_3 layer, the adsorbed CO was oxidized by oxygen (in either dry gas phase or aqueous phase), during which ATR-IR spectra were recorded. The normalized integrated peak area of linearly adsorbed CO during oxidation is shown in Fig. 5 as a function of time for both the gas and aqueous phase (pH 6.9). In both experiments, an immediate decrease in the peak intensity of linear and bridging CO was observed during oxidation of preadsorbed CO, but no CO_2 was detected. Chromatic effects are absent in this experiment, because of the high amount of oxygen in the feed compared with the amount of platinum present on the IRE.

The initial rate of disappearance of adsorbed CO was the lowest in gas phase and approximately doubled in aqueous phase. After flowing oxygen in water for 10 min, 98% of the CO was oxidized; in comparison, only 65% of the CO was oxidized in gas phase after 10 min. The initial rate of disappearance of adsorbed CO in aqueous phase was also investigated at different pH values (Fig. 6), each point indicates an individual experiment at a specific pH and the experiments were performed randomly. As a reference, the gas-phase oxidation rate is indicated as a horizontal line.

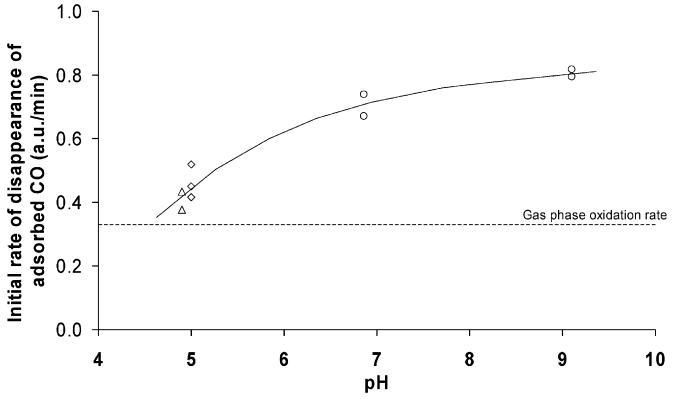

Fig. 6. Initial rate of disappearance of preadsorbed CO in aqueous phase as a function of pH (integrated peak area for linear CO/min) ((△) adjusted with H_3PO_4, (◇) adjusted with H_2SO_4, (○) adjusted with NaOH).

Clearly, the initial rate of disappearance of adsorbed CO increased with increasing pH, and the rates were always higher in aqueous phase than in gas phase.

4. Discussion

4.1. Catalyst characterization

The applied method of catalyst immobilisation on an IRE evidently resulted in a stable catalyst layer when applied for days in flowing aqueous solutions. Although preparation of stable layers of supported catalyst for ATR-IR has been reported by evaporation of a aqueous suspension of the catalyst powder on the IRE without further treatment [6,9,11], replication of this treatment in our laboratory did not result in stable layers when water was flushed. The modified method reported here—application of colloidal alumina, followed by calcination and reduction to immobilize the catalyst layer—resulted in a very smooth and stable Pt/Al_2O_3 layer, without influencing the properties of the catalyst, which could be used repeatedly.

4.2. CO adsorption from gas and aqueous phase

Adsorption of CO from gas or aqueous phase on the same catalyst sample revealed clear differences, as can be seen by comparison of Figs. 2 and 3. CO adsorption from aqueous phase results in a CO red shift of 47 cm^{-1} compared with dry gas-phase adsorption. Moreover, the IR absorbance increased approximately fourfold. Third, the ratio of integrated intensities for linear and bridging CO (L/B ratio) decreased from 6.9 in gas phase to 4.1 in aqueous phase.

The observed red shift in the presence of water is in accordance with several other studies reporting shifts to lower wavenumber of 11–34 cm^{-1} [9]. Various single-crystal studies have reported the influence of water on adsorbed CO [10,12,31]. The spectral properties of adsorbed CO is altered by the presence of heavy water for both Pt(100) and Pt(111) [10,12]. A clear red shift was observed for both linear and bridging CO on platinum on gradual addition of D_2O, attributed to a combination of increased π-back-donation from Pt to CO together with a change in CO dipole moment [10,12]. For a differently pretreated $Pt–Al_2O_3$ sample, CO was adsorbed from CH_2Cl_2, and linear adsorbed CO on Pt was found between 2030 and 2058 cm^{-1}, depending on the pretreatment procedure [8]. Unfortunately, no gas-phase spectra were shown in that study, so the effect of the solvent could not be estimated for that particular sample. Nevertheless, the authors did report large Pt particles (6 nm), for which it is generally accepted that gas-phase CO adsorption leads to bands at around 2070–2090 cm^{-1} [15,28–30]. As such, it seems that CH_2Cl_2 also induced a shift in the CO stretch frequency. This suggests for both water and CH_2Cl_2 the possibility of a direct interaction between solvent molecules and adsorbed CO, most likely via hydrogen bonding. Preliminary calculations, however, show that co-adsorption of water has a more distinct effect on the CO peak position than does formation of hydrogen bonds [32].

In the field of catalyst characterization, it is well known that with increasing support alkalinity, the red shift of linearly and bridging CO is accompanied by a lower linear to bridge ratio due to the increased back-donation from the noble metal particles [20,24,33,34]. In the present study, the linear-to-bridge ratio shows a clear decrease from 6.9 to 4.1 when the CO bands shifts to lower wavenumber. Based on the red shift and altered L/B ratio, no distinction can be made between a direct effect of water on the CO molecule and an indirect effect via modification of the metal particle potential, inducing increased back-donation from the metal to CO, or a combination of both phenomena.

Remarkably, the CO intensity increased about fourfold when adsorbed from aqueous phase compared with gas phase. This observation is similar to previous results of a fivefold-greater intensity for CO on Pt/ZnSe, comparing CO adsorption from aqueous phase with gas phase [7]. Unfortunately, papers reporting on changes in intensity with the addition of water are scarce.

At first instance, it seems likely that the increased intensity could be caused by a greater penetration depth, which depends on the refractive index of the sample on top of the IRE [5]. In general, the refractive index of a porous material can be calculated from the individual refractive indices of the porous material and the surrounding medium [35]. Calculations showed that changing the medium from gas to water increases the penetration depth only 1.29-fold (see supplementary information), which is significantly less than the fourfold increase in intensity.

A greater CO coverage in aqueous phase also can be excluded as a cause of the higher IR intensity, because CO is well known to adsorb strongly on platinum, and full coverage is easily reached in gas phase at 1 atm. For this reason, CO chemisorption is often used to determine metal particle dispersion [36]. Therefore, it is impossible for aqueous-phase CO adsorption to lead to a fourfold-greater coverage compared with gas-phase adsorption.

A possible remaining explanation for the increased intensity is a change in the extinction coefficient with the addition of water. Adsorption of wetted CO (with water vapor) on Pt/Al_2O_3 did not change the extinction coefficient of adsorbed CO [15].

However, the addition of bulk water showed a dramatic effect on the intensity of adsorbed CO, similar to that found in the present study [7]. For this reason, we propose that the surrounding of adsorbed CO by an excess of water molecules results in polarization of the CO molecule via, for example, hydrogen bonding, which directly affects its extinction coefficient due to an increased transition dipole moment.

In addition, the stretch frequency of linearly CO adsorbed on Pt/Al_2O_3 was found to shift down with increasing pH, as shown in Fig. 4B. In electrochemistry, it is well known that a change in electrode potential causes a shift in peak position of adsorbed CO [37–39]. Moreover, a linear relationship between pH of the solution and the observed metal potential has been reported [40], accompanied by a relationship between the corrected potential and the observed frequency of adsorbed CO [37,41]. Unfortunately, comparing those results directly with those of the present study is difficult, because of the applied potential in electrochemistry. In fact, to do so, we would need IR spectra of adsorbed CO at an open circuit potential of a reacting electrode, which, to the best of our knowledge, are not available due to severe mass transfer problems. In gas-phase chemistry, the stretch frequency of adsorbed CO is considered a sensitive probe of metal–support interactions [13–24], which are known to influence the electronic properties of the supported metal and thereby its catalytic activity [18]. As a final point, a strong direct effect of pH on the CO stretch frequency (through, e.g., the formation of a $CO–H^+$ adduct) can be excluded. Such adduct formation would result in a weakening of the CO bond, resulting in a shift to lower frequency with decreasing pH. However, exactly the opposite trend is observed.

In conclusion, we attribute all of the observed spectral differences in gas-phase and aqueous-phase adsorption at different pH values (i.e., the red shifts, decreased L/B ratio, and fourfold increased intensity) to a combination of increased back-donation from the supported metal and a direct effect of water on the transition dipole moment of adsorbed CO.

4.3. Oxidation of preadsorbed CO in gas and aqueous phase

Fig. 5 clearly shows an increased rate of disappearance of adsorbed CO in aqueous phase compared with that in the gas-phase oxidation experiment. In addition, increasing pH from 4.9 to 9.1 significantly enhanced the CO oxidation rate. Similarly, we recently showed that the oxidation rate of preadsorbed CO on Pt/ZnSe was about twice as fast in aqueous phase than in gas phase at neutral pH [7]. Electro-oxidation of CO over either platinum or gold in acidic and alkaline solutions was found to be fastest in alkaline solutions in which the CO stretch frequency was lowest [40,41], in agreement with our findings. Moreover, the stretch frequency of adsorbed CO can be linearly related to the CO oxidation rate, as depicted in Fig. 7. This linear relationship points to an effect of metal particle potential on the rate-determining step of CO oxidation in aqueous phase.

For gas-phase CO oxidation, in zeolite-supported catalysts higher CO activity was found in the samples with CO bands at lower wavenumbers, accompanied by a lower L/B ratio [24]. Based on XAFS experiments, the authors of that study attributed the increased oxidation activity to increased electron density on the metal particles. The increased potential induces a higher π-back-donation from the metal particle to CO, resulting in a red shift of the CO stretch frequency and a lower L/B ratio. Similar trends were observed for sulphur-poisoned Pt/SiO_2 catalysts [42]. We show here for the first time that the same relationship holds for CO oxidation over Pt/Al_2O_3 in aqueous phase. In gas-phase experiments, the red shift is normally accompanied by a decreased L/B ratio, which is observed only when comparing the gas-phase and aqueous-phase experiments in the present study. No significant difference in L/B ratio was found with changing pH. However, in gas phase, the reported shifts in band position are much larger (up to 100 cm^{-1}) than in our study (13 cm^{-1} at pH 4.9–9.1). The increased π-back-donation weakens the C–O bond by supplying electrons in the antibonding orbital [43], which will be more reactive toward the p electrons of adsorbed oxygen atoms. As a result, the CO molecule is more easily oxidized with increasing pH.

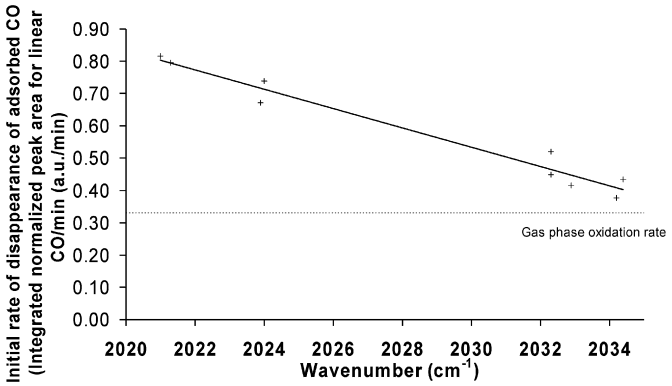

Fig. 7. Initial rate of disappearance of preadsorbed CO in aqueous phase as a function of infrared frequency of linearly adsorbed CO on Pt/Al_2O_3; for comparison, gas phase oxidation rate is indicated with the dotted line.

From this perspective, it is also interesting to extrapolate the found linear relationship to the gas-phase oxidation rate indicated in Fig. 7. The two lines intercept at 2037 cm^{-1}, which is significantly lower than the observed frequency for adsorbed CO in gas phase (2071 cm^{-1}). This observation demonstrates that the linear relation between peak position and oxidation rate cannot be universally applied. The most likely explanation for this is a change of mechanism in the presence of water. For a given mechanism, the CO band position can be directly related to the oxidation activity, as shown in Fig. 7 and published in the literature for gas-phase oxidation [24].

It is well accepted that the mechanism for CO oxidation in gas phase on platinum catalysts proceeds via a three-step Langmuir–Hinselwood reaction mechanism in which adsorbed CO reacts with dissociatively adsorbed oxygen (Table 1) [44,45]. In addition, CO oxidation in aqueous phase has been examined extensively in electrochemistry [10,37,40,46–48]. The oxygen-containing species for electro-oxidation is thought to result from oxidation of water at the electrode surface and is usually considered to be adsorbed OH [46,48]. An activated complex, such as adsorbed $CO–H_2O$ on platinum, which forms

Table 1
Proposed reaction mechanism of CO and O_2 in gas phase and aqueous phase[a]

Gas phase [44,45]	Aqueous phase [this paper]
$CO + \star \rightleftharpoons CO^\star$	$CO + \star \rightleftharpoons CO^\star$
$O_2 + 2^\star \rightleftharpoons 2O^\star$	$CO^\star + yH_2O(l) \rightleftharpoons [(CO)\cdot(H_2O)_y]^\star$
$O^\star + CO^\star \rightleftharpoons CO_2 + 2^\star$	$O_2 + 2^\star \rightleftharpoons 2O^\star$
	$O^\star + [(CO)\cdot(H_2O)_y]^\star \rightleftharpoons CO_2 + yH_2O(l) + 2^\star$

[a] $\star$ signifies a platinum site, and $X^\star$ an adsorbed specie on platinum.

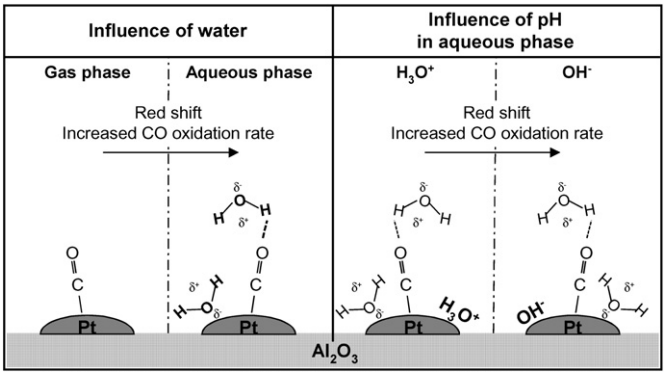

Fig. 8. Schematic presentation of the influence of water and pH on the CO stretch frequency and CO oxidation rate (more details can be found in the text).

CO–OH during oxidation [46], also has been proposed. Because in the present study the oxidation of CO on Pt/Al_2O_3 in aqueous phase did not occur in the absence of O_2, we can exclude the formation of OH from water on the platinum surface. This is in agreement with DFT calculations showing that during CO oxidation in water over Pt(111), water could not dissociate on uncharged Pt(111) [49]. Moreover, in heterogeneous catalysis, it is well known that water does not dissociate on platinum particles in the water–gas shift or steam reforming at high temperatures.

Obviously, the reaction mechanism of CO oxidation by O_2 over Pt/Al_2O_3 in aqueous phase is not only different from gas-phase oxidation, but also from electro-chemical oxidation, in which water is generally accepted as the oxygen source, electrons are removed via the electrode, and the reaction can be performed in the absence of dissolved molecular oxygen. Because the adsorption of CO from aqueous phase already revealed a direct effect of liquid water on the CO molecules (reflected in a higher extinction coefficient, vide ante), we propose an activated complex of CO molecules and water, $[(CO)\cdot(H_2O)_y]^\star$, as a reaction intermediate for CO oxidation by O_2 in aqueous phase (Table 1). Due to hydration of the adsorbed CO molecule, the CO bond is weakened significantly, as reflected in the large red shift and decreased L/B ratio, which facilitates its oxidation. The exact configuration of the CO–water complex remains unclear and is currently subject of ongoing theoretical calculations. Moreover, an effect of water on adsorbed dissociated oxygen cannot be excluded.

Finally, Fig. 8 summarizes the findings of this study. The presence of co-adsorbed and bulk water affect the metal particle potential and the CO transition dipole moment, respectively, most likely by complex formation between CO and H_2O. This interaction alters the reaction mechanism and rate of CO oxidation. In addition, the pH mainly affects the CO molecule via a potential change of the metal particle, which in turn is directly related to the observed rate of oxidation.

5. Conclusion

This study convincingly shows the benefit of ATR-IR spectroscopy for comparing properties of adsorbed molecules on supported noble metal catalysts in gas phase and aqueous phase, because the same catalyst can be used for both types of experiments. The aqueous solution significantly influences the properties of CO adsorbed on Pt/Al_2O_3. A large red shift, a decreased L/B ratio, and a fourfold-increased intensity are observed, resulting from a combination of increased back-donation from the metal and a direct effect of water on the transition dipole moment of adsorbed CO. As a result, the reaction mechanism is altered by the presence of liquid water compared with gas-phase or electro-chemical CO oxidation. The effect of pH on the CO oxidation rate can be attributed to a potential change in the metal particles, which in turn affects the CO stretch frequency, which is linearly related to the oxidation rate.

Acknowledgments

This work was supported by DSM Research, the Netherlands, and performed under the auspices of the Dutch Institute for Research in Catalysis (NIOK).

Supporting information

The online version of this article contains additional supporting information.

Please visit doi:10.1016/j.jcat.2006.11.019.

References

[1] P.T. Anastas, L.G. Heine, T.C. Williamson, Green Chemical Syntheses and Processes, Am. Chem. Soc., Washington, DC, 2000.
[2] A. Pintar, Catal. Today 77 (2003) 451.
[3] A. Kapoor, T. Viraraghavan, J. Environ. Eng. 123 (1997) 371.
[4] Y.I. Matatov-Meytal, M. Sheintuch, Ind. Eng. Chem. Res. 37 (1998) 309.
[5] N.J. Harrick, Internal Reflection Spectroscopy, Interscience, New York, 1967.
[6] T. Bürgi, A. Baiker, J. Phys. Chem. B 106 (2002) 10649.
[7] S.D. Ebbesen, B.L. Mojet, L. Lefferts, Langmuir 22 (2006) 1079.
[8] D. Ferri, T. Bürgi, A. Baiker, J. Phys. Chem. B 105 (2001) 3187.
[9] R. He, R.R. Davda, J.A. Dumesic, J. Phys. Chem. B 109 (2005) 2810.
[10] N. Kizhakevariam, X. Jiang, M.J. Weaver, J. Chem. Phys. 100 (1994) 6750.
[11] I. Ortiz-Hernandez, C.T. Williams, Langmuir 19 (2003) 2956.
[12] N.C. Yee, G.S. Chottiner, D.A. Scherson, J. Phys. Chem. B 109 (2005) 7610.
[13] M. Bartok, J. Sakany, A. Sitkei, J. Catal. 72 (1981) 236.
[14] S. Boujana, D. Demri, J. Cressely, A. Kiennemann, J.P. Hindermann, Catal. Lett. 7 (1990) 359.
[15] A. Bourane, O. Dulaurent, D. Bianchi, Langmuir 17 (2001) 5496.
[16] D.C. Koningsberger, D.E. Ramaker, J.T. Miller, J. de Graaf, B.L. Mojet, Top. Catal. 15 (2001) 35.

[17] G. Larsen, G.L. Haller, Catal. Lett. 3 (1989) 103.
[18] B.L. Mojet, J.T. Miller, D.E. Ramaker, D.C. Koningsberger, J. Catal. 186 (1999) 373.
[19] B.L. Mojet, D.C. Koningsberger, Catal. Lett. 39 (1996) 191.
[20] B.L. Mojet, J.T. Miller, D.C. Koningsberger, J. Phys. Chem. B 103 (1999) 2724.
[21] V. Pitchon, M. Primet, H. Praliaud, Appl. Catal. 62 (1990) 317.
[22] M. Primet, J. Catal. 88 (1984) 273.
[23] F. Stoop, F.J.C.M. Toolenaar, V. Ponec, J. Catal. 73 (1982) 50.
[24] T. Visser, T.A. Nijhuis, A.M.J. van der Eerden, K. Jenken, Y. Ji, W. Bras, S. Nikitenko, Y. Ikeda, M. Lepage, B.M. Weckhuysen, J. Phys. Chem. B 109 (2005) 3822.
[25] T.A. Nijhuis, A.E.W. Beers, T. Vergunst, I. Hoek, F. Kapteijn, J. Moulijn, Catal. Rev. Sci. Eng. 43 (2001) 345.
[26] J.E. Benson, H.S. Hwang, M. Boudart, J. Catal. 4 (1965) 704.
[27] E.V. Benvenutti, L. Franken, C. Moro, Langmuir 15 (1999) 8140.
[28] A. Bourane, O. Dulaurent, D. Bianchi, J. Catal. 196 (2000) 115.
[29] R. Barth, R. Pitchai, R.L. Anderson, X. Verykios, J. Catal. 116 (1989) 61.
[30] A. Bourane, D. Bianchi, J. Catal. 220 (2003) 3.
[31] G. Rupprechter, T. Dellwig, H. Unterhalt, H.J. Freund, J. Phys. Chem. B 105 (2001) 3797.
[32] M. Neurock, Personal communication, unpublished results, University of Virginia, Department of Chemical Engineering, Charlottesville, USA (May 2006).
[33] M.J. Kappers, M. Vaarkamp, J.T. Miller, F.S. Modica, M.K. Barr, J.H. Vandermaas, D.C. Koningsberger, Catal. Lett. 21 (1993) 235.
[34] D.E. Ramaker, J. de Graaf, J.A.R. van Veen, D.C. Koningsberger, J. Catal. 203 (2001) 7.
[35] M.M. Braun, L. Pilon, Thin Solid Films 496 (2006) 505.
[36] M. Primet, M. El Azhar, R. Frety, M. Guenin, Appl. Catal. 59 (1990) 153.
[37] S.-C. Chang, M.J. Weaver, J. Chem. Phys. 92 (1990) 4582.
[38] S.A. Wasileski, M.T.M. Koper, M.J. Weaver, J. Phys. Chem. B 105 (2001) 3518.
[39] J. Xu, J.T. Yates, Surf. Sci. 327 (1995) 193.
[40] A. Couto, A. Rincón, M.C. Pérez, C. Gutiérrez, Electrochim. Acta 46 (2001) 1285.
[41] K. Kunimatsu, A. Aramata, H. Nakajima, H. Kita, J. Electroanal. Chem. 207 (1986) 293.
[42] F.J. Gracia, S. Guerrero, E.E. Wolf, J.T. Miller, A.J. Kropf, J. Catal. 233 (2005) 372.
[43] G. Blyholder, J. Phys. Chem. 68 (1964) 2772.
[44] G. Ertl, T. Engel, Adv. Catal. 28 (1979) 1.
[45] G. Ertl, Adv. Catal. 37 (1990) 213.
[46] S. Gilman, J. Phys. Chem. 68 (1964) 70.
[47] H.L. Lam-Wing, A. Wieckowski, M.J. Weaver, J. Phys. Chem. 92 (1988) 6985.
[48] N.P. Lebedeva, A. Rodes, J.M. Feliu, M.T.M. Koper, R.A. van Santen, J. Phys. Chem. B 106 (2002) 9863.
[49] S. Desai, M. Neurock, Electrochim. Acta 48 (2003) 3759.